Proceedings of the 20th International Conference on Soil Mechanics and Geotechnical Engineering– Rahman and Jaksa (Eds)

Practical reliability-based approach for liquefaction vulnerability

Approche Pratique Basée sur la Fiabilité Pour la Vulnérabilité à la Liquéfaction

Vipman Tandjiria
Tunnel and Ground Engineering, Jacobs, Australia, vipman.tandjiria@jacobs.com

ABSTRACT: A probabilitybased approach is considered important as the deterministic approach cannot explicitly reflect the uncertainties of engineering properties of liquefied soils. The objective of this paper is to propose a practical reliability-based approach for evaluating the liquefaction vulnerability using object-oriented constrained optimization, coupled with a semi-empirical procedure. The reliability analysis is carried out using the Hasofer-Lind index (1974) in the design space of random variables. A non-linear optimisation model is derived by minimising the Hasofer-Lind reliability index by considering random parameters, such as soil density, depth of groundwater table, CPT cone resistance, and correction of fines content, subject to a liquefaction potential index (LPI) category constraint. The results presented in this paper demonstrate that the proposed probabilistic approach, coupled with an empirical solution, is an efficient procedure to determine the probability of liquefaction vulnerability. The approach was applied to an historical case of liquefaction in Christchurch, New Zealand. Figures showing cumulative distribution function (CDF), calculated from reliability indices, versus LPI are presented.

RÉSUMÉ : Une approche probabiliste est considérée importante parce-que l'approche déterministe ne peut pas refléter explicitement la nature des tremblements de terre et les propriétés techniques des sols liquéfiés. L'objectif de cet article est de développer une approche pratique basée sur la fiabilité pour évaluer la vulnérabilité à la liquéfaction en utilisant l'application d'une analyse pratique basée sur la fiabilité utilisant l'optimisation sous contraintes orientées objet, associée à une procédure semi-empirique. L'analyse de fiabilité est effectué à l'aide de l'indice de fiabilité de Hasofer-Lind (1974) dans l'espace de conception des variables aléatoires. Un modèle d'optimisation non linéaire est dérivé en minimisant l'indice de fiabilité Hasofer-Lind en considérant des paramètres aléatoires , tels que la densité du sol, la nappe phréatique, la résistance du cône CPT et la correction de la teneur en fines, sous réserve d'une contrainte de catégorie d'indice de potentiel de liquéfaction (LPI). Les résultats présentés dans cet article démontrent que l'approche probabiliste proposée, couplée à une solution empirique, est une procédure efficace pour déterminer la probabilité de vulnérabilité à la liquéfaction. L'approche a été appliquée à un cas historique de liquéfaction à Christchurch, Nouvelle-Zélande. Les figures de la fonction de distribution cumulative (CDF), calculées à partir des indices de fiabilité, par rapport à LPI sont présentées.

KEYWORDS: Liquefaction, reliability, liquefaction potential index, liquefaction vulnerability.

1 INTRODUCTION

Soil liquefaction is one of the main considerations by geotechnical engineers in countries or regions susceptible to earthquakes. Soil liquefaction following an earthquake event often causes damage to structures and infrastructure. It occurs when soils are under rapid cyclic shearing stresses, as in an earthquake event. This causes an increase in pore water pressures and reduction in effective stress, which results in loose saturated or partially saturated granular soils contracting and losing their strength.

Semi-empirical procedures for evaluating liquefaction potential during earthquakes, based on field performance case histories of cone penetration test (CPT) data and standard penetration test (SPT) data, have been developed during the last five decades, pioneered by Seed and Idriss (1971). Since then, these semi-empirical procedures have evolved and been improved (e.g. Zhang et al. 2002, Idriss and Boulanger 2006, Boulanger and Idriss 2014). Improvements include updated liquefaction case histories from recent earthquake events, and the introduction of correction factors related to fines content and grain characteristics of the liquefied soils. These procedures are now generally considered as standard practice to evaluate the liquefaction resistance of soils.

Most of the above procedures are based on a deterministic approach, derived from theoretical considerations with support from experimental data. The deterministic approach cannot explicitly reflect the uncertainties inherent in the engineering properties of liquefied soils. Only a limited amount of research that considers probabilistic procedures to evaluate liquefaction potential has been carried out (e.g. Cetin et al. 2002, Moss et al. 2006, Idriss and Boulanger 2008, Boulanger and Idriss 2014).

Moss et al. (2006) presented a probabilistic method to locate the threshold of liquefaction triggering using engineering statistics, Bayesian updating, and reliability methods. The probability problem is defined using a limit state function where load and resistance values are equal. The testing of the limit state function against the data is defined through Bayesian updating. As a result, plots of contours of probability of liquefaction as a function of the equivalent uniform cyclic stress ratio (CSR) and the modified normalised CPT tip resistance can be produced.

Idriss and Boulanger (2008) studied a probabilistic method using CPT-based liquefaction triggering correlated with an updated case history database, revised Magnitude Scaling Factor (MSF) relationship and maximum likelihood method utilising the forms of the limit state and likelihood functions proposed by Cetin et al. (2002). A similar procedure was used by Boulanger and Idriss (2014) with an updated case history database. The limit state function, which is the difference between the natural logs of the cyclic resistance ratio (CRR) and CSR, should be less than zero to cause liquefaction. Note that the uncertainty in the liquefaction triggering model proposed here is conditional, including only the model uncertainty. The result of the latter study shows that, by assuming 16% probability of liquefaction, the calculated correlation agrees with the deterministic liquefaction triggering correlation.

Besides the liquefaction triggering model (both deterministic or probabilistic correlation), uncertainties in seismic hazard and site characterization are still considered two most important factors in probabilistic assessment (Idriss and Boulanger 2014). In addition to this, random variables like soil density, depth of groundwater table, CPT cone resistance data, and correction of fines content are also crucial in evaluating liquefaction potential.

It is widely understood that the liquefaction triggering model alone cannot capture liquefaction induced damage due to an earthquake event. Other factors like depths and thickness of liquefying soil, and presence or absence of non-liquefying crust affect the vulnerability of land to liquefaction. For these reasons,

another measured index to predict the impact of liquefaction at ground surface is required. This will be discussed in Section 3.

This paper presents a reliability-based approach, combined with the available semi-empirical procedure, for evaluating liquefaction potential to estimate probability of land damage associated with an earthquake.

2 LIQUEFACTION TRIGGERING

The liquefaction triggering procedures based on CPT, proposed by Boulanger and Idriss (2014), were chosen in this study and a brief summary is provided in this section.

In evaluating liquefaction potential, CPT is more widely used in engineering practice than other methods (SPT, shear-wave velocity measurements, and Becker penetration test/BPT). CPT has the advantages of a continuous stratigraphic profile of cone resistance (q_c) and the fact that CPT works can be carried out in a short time and at relatively low cost.

The liquefaction triggering procedure basically involves the following:

- Calculation of earthquake-induced CSR/seismic demand;
- Calculation of CRR/earthquake capacity; and
- Calculation of factor of safety (FoS) against liquefaction which is the ratio of CRR to CSR. When FoS is greater than one means the investigated specific soil layer should not liquefy. On the other hand, when FoS is less than 1, liquefaction is likely to occur within that soil layer.

2.1 *Earthquake-induced CSR*

The equivalent uniform CSR at earthquake magnitude of 7.5 and effective vertical stress of 1 atm is calculated using eq. 1 below.

$$CSR_{M=7.5,\sigma_v'=1} = 0.65\,\frac{\sigma_v}{\sigma_v'}\frac{a_{max}}{g} r_d \frac{1}{MSF}\frac{1}{K_\sigma} \quad (1)$$

Where:

σ_v = vertical total stress
σ_v' = vertical effective stress
a_{max}/g = ground surface maximum horizontal acceleration
r_d = shear stress reduction factor
MSF = earthquake magnitude scaling factor
K_σ = effective overburden stress factor

The parameter r_d is expressed below

$$r_d = \exp[\alpha(z) + \beta(z)\cdot M] \quad (2)$$

$$\alpha(z) = -1.012 - 1.126\sin\left(\frac{z}{11.73} + 5.133\right) \quad (2a)$$

$$\beta(z) = 0.106 - 0.118\sin\left(\frac{z}{11.28} + 5.142\right) \quad (2b)$$

z is depth below the ground surface in meters. The arguments inside the brackets are in radians.

MSF is a function of earthquake magnitude, M as follows:

$$MSF = 6.9.\exp\left(\frac{-M}{4}\right) - 0.058 \le 1.8 \quad (3)$$

The effective overburden correction factor, K_σ, is expressed in terms of the corrected cone resistance, q_{c1Ncs}, which is the resistance for a similar sand at an effective overburden stress of 1 atm (P_a).

$$K_\sigma = 1 - C_\sigma \ln\left(\frac{\sigma_v}{P_a}\right) \le 1.1 \quad (4)$$

$$C_\sigma = \frac{1}{37.3 - 8.27(q_{C1NCS})^{0.264}} \le 0.3 \quad (4a)$$

Where

$$q_{C1NCS} = q_{C1N} + \Delta q_{C1N} \quad (5)$$

q_{c1N} values are CPT resistances corrected for overburden stress expressed below

$$q_{C1N} = C_N \frac{q_c}{P_a} \quad (6)$$

with

$$C_N = \left(\frac{P_a}{\sigma_v'}\right)^m \le 1.7 \quad (6a)$$

$$m = 1.338 - 0.249(q_{C1NCS})^{0.264} \quad (6b)$$

The equivalent clean sand adjustment for CPT is expressed below:

$$\Delta q_{C1N} = \left(11.9 + \frac{q_{C1N}}{14.6}\right)\exp\left(1.63 - \frac{9.7}{FC+2} - \left(\frac{15.7}{FC+2}\right)^2\right) \quad (7)$$

Where FC is the percent fines content. FC will affect the liquefaction triggering correlation charts. Soil with larger fines content will shift the correlation charts to the left and thus tend to be less susceptible to liquefaction. Unless FC is obtained from laboratory testing, FC of the assessed materials is estimated by its relationship with the soil behavior type index, I_c expressed in eq. 8.

$$I_C = \frac{(FC+137)}{80} + \varepsilon \quad (8)$$

Where ε is an error term to represent a correction to fines content. Boulanger and Idriss (2014) suggested that ε has a mean and standard deviation of 0 and 0.29, respectively.

I_c is calculated using the equations proposed by Robertson and Wride (1998).

Note that iterative procedures are required to define the corrected cone resistance, q_{c1Ncs} (refer eqs. 4, 5, 6 and 7).

2.2 *CRR*

Boulanger and Idriss (2014) proposed a revised deterministic CPT-based correlation for CRR in terms of q_{c1Ncs}. The proposed correlation was developed based on different values of FC by incorporating additional recent case histories including a series of earthquakes which occurred in Christchurch, New Zealand in the period from 4th September 2010 to 23rd December 2011. The revised correlation is expressed in equation 9 below.

$$CRR_{M=7.5,\sigma_v'=1} = \exp\left(\frac{q_{c1NCS}}{113} + \left(\frac{q_{c1NCS}}{1000}\right)^2 - \left(\frac{q_{c1NCS}}{140}\right)^3 + \left(\frac{q_{c1NCS}}{113}\right)^4 - 2.8\right) \quad (9)$$

3 LIQUEFACTION POTENTIAL INDEX (LPI)

Iwasaki et al. (1978) introduced a Liquefaction Potential Index (LPI) that can be used to predict the severity or damage potential of liquefaction of a site. This index basically accounts for the depths of liquefied layers by introducing a weighting function applied to each soil layer, and its estimated factor of safety (FoS) obtained from a liquefaction triggering approach.

Since then, several methods of liquefaction vulnerability have been proposed to improve the original LPI proposed by Iwasaki et al. (1978). The two most well-known methods are the Ishihara inspired LPI (LPI_{ISH}) method developed by Maurer et al. (2015) and the Liquefaction Severity Number (LSN) method developed by Tonkin & Taylor (2013).

In this study, LPI_{ISH} is chosen due to its straightforward expression, while the determination of LSN requires the

calculation of the volumetric reconsolidation strain in each layer. Since the proposed reliability-based approach for liquefaction vulnerability proposed in this study is the first effort to be combined with the liquefaction triggering approach, an option to use the LSN method will be considered for a further study.

Maurer et al. (2015) proposed an improved functional form of the original LPI_{ISH} by incorporating the effect of a non-liquefied surface layer on liquefaction vulnerability. The original LPI_{ISH} was found to be inaccurate in predicting liquefaction vulnerability with field data from many earthquakes.

The LPI_{ISH} method, also known as the new Ishihara-inspired index, was based on the Ishihara (1985) boundary curve separating liquefaction cases from non-liquefaction cases that is assumed to have a similar threshold LPI value, presented in terms of thickness of non-liquefying surface layer and thickness of liquefying sand layer.

For simplicity, the remainder of this paper will use LPI to represent the new LPI_{ISH} as expressed in eq. 10.

$$LPI = \int_{H_1}^{z_L} f(FS)\frac{25.56}{z}dz \tag{10}$$

Where

$$f(FS) = (1 - FS) \quad if\ [(FS \le 1) \cap (H_1.m(FS) \le 3)]$$

$$else\ f(FS) = 0 \tag{10a}$$

and

$$m(FS) = \exp\left(\frac{5}{25.56(1-FS)}\right) - 1 \tag{10b}$$

Where H_1 is the depth of non-liquefying crust layer and z_L is the total depth of the assessed soils that is limited to 20 m. FS is the factor of safety (FoS) defined in Section 2.

The threshold LPI values proposed by Iwasaki et al. (1978) to assess liquefaction induced damage have been broadly used to characterize liquefaction vulnerability in many liquefaction case studies. Based on that, the threshold LPI values adopted in this study are summarized in Table 1.

Table 1. Threshold LPI values

Damage classification	Expected LPI Range
No liquefaction	LPI < 4
Marginal liquefaction	4 ≤ LPI < 8
Moderate liquefaction	8 ≤ LPI < 15
Severe liquefaction	15 ≤ LPI

4 HASOFER-LIND RELIABILITY INDEX

The reliability index is one of the effective indices for the reliability of a system. This section discusses the reliability-based design using the Hasofer-Lind index (1974) in the design space of random variables. The method has been used for probabilistic analysis in geotechnical engineering (e.g. Low and Tang 1997, Tandjiria et al. 2000, Low et al. 2001).

Low and Tang (1997) carried out automated reliability analysis of footing foundations. Tandjiria et al. (2000) carried out reliability analysis of laterally loaded piles by combining the Hasofer-Lind index with a response surface method. Low et al. (2001) studied reliability-based design of a semi-gravity retaining wall and anchored or propped walls.

The Hasofer-Lind reliability index, β, (Ditlevsen 1981) is expressed below

$$\beta = \min_{X \in F} \sqrt{(X-\mu)^T C^{-1} (X-\mu)} \tag{11}$$

or in a matrix formulation

$$\beta = \min_{X \in F} \sqrt{\left[\frac{x_i - m_i}{\sigma_i}\right]^T [R]^{-1} \left[\frac{x_i - m_i}{\sigma_i}\right]} \tag{12}$$

Where

F = The limit state boundary separating the domain of satisfactory performance from the domain of unsatisfactory performance
X = A vector representing the set of random variables
μ = A vector representing the means of the random variables
C = The covariance matrix of random variables
x_i, m_i and σ_i correspond to the randomly assigned value, mean and standard deviation of each random variable

Figure 1 shows an illustration of β in units of directional standard deviations of an expanding ellipsoid for two random variables. For n random variables, Eqs. 11 and 12 form a hyper-ellipsoid in n-dimensional space. β is defined as the shortest distance in units of directional standard deviation from the mean value point of the random variables to a limit state boundary.

The limit state boundary is represented by a performance function. When the performance function can be explicitly expressed in terms of the random variables (e.g. for the case of liquefaction in this paper), reliability index calculation is straight forward. However, when the performance function is implicitly connected to the random variables, an alternative approach to integrate with the random variables is required. One such approach is to use response surface methods (Tandjiria et al. 2000).

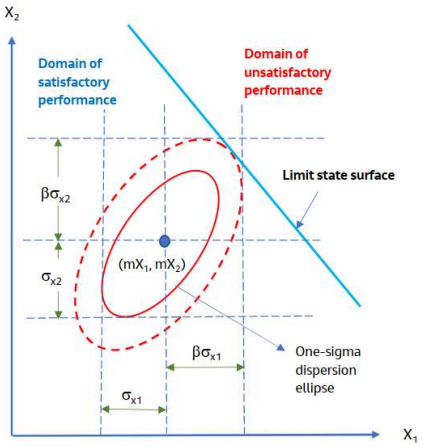

Figure 1. Reliability Index β illustrated in two random variables.

As the quadratic form in eq.12 has a negative exponent of the multivariate normal probability density function (PDF), minimizing β is to maximize the value of the multivariate normal PDF and find the smallest ellipsoid tangent to the limit state surface.

5 APPLICATION OF RELIABILITY-BASED APPROACH TO LIQUEFACTION CASE

Calculations of triggering analysis, LPI and object-oriented constrained optimization in this study were carried out using a spreadsheet platform (i.e. Microsoft® Excel).

The proposed reliability-based approach was applied to reassess liquefaction vulnerability of a real liquefaction case at a site in Christchurch, South Island, New Zealand.

5.1 *General information of Christchurch earthquake*

Christchurch, located in the Canterbury region of New Zealand, was shaken by a series of medium to large earthquakes between September 2010 and December 2011. The recorded magnitudes were between Mw 5.6 and Mw 7.1 (Tonkin & Taylor 2013). The largest earthquake with a magnitude of Mw 7.1 occurred on 4th September 2010 with its epicenter approximately 10 km below (focal depth) and about 40 km west of Christchurch. Two following major earthquakes (Mw 6.3 and Mw 6.0) occurred on 22nd February and 13th June 2011.

These earthquakes caused liquefaction, lateral spreading and ground surface subsidence in Christchurch with widespread damage to buildings, residential homes, land and infrastructure.

Following these events, agencies including the New Zealand Government through the Ministry of Building, Innovation and Employment (MBIE), universities in New Zealand and several international groups such as Geo-engineering Extreme Event Reconnaissance USA and the Japanese Geotechnical Society (JGS) conducted reconnaissance survey and collected post-liquefaction data. Most works were documented and published in technical papers (e.g. Cubrinovski et al. 2010, MBIE 2012, Tonkin & Taylor 2013).

MBIE's guidance document (MBIE 2012) has classified three technical categories of land in Canterbury under future major earthquakes as follows:

Table 2. MBIE technical category classification

Technical Category	Future performance from liquefaction	Nominal SLS land settlement	Nominal ULS land settlement
TC1	Damage is unlikely in future major earthquake	0 – 15 mm	0 – 25 mm
TC2	Damage is possible in a future major earthquake	0 – 50 mm	0 – 100 mm
TC3	Damage is probable in a future major earthquake	>50 mm	>100 mm

Furthermore, another critical area called the "red zone" (CERA 2012) was also classified. This area experienced very bad damage and required a long period of reconstruction works.

Figure 2 shows the red zone area, the areas of the three technical categories, and CPT locations. Data from the three CPT locations on the figure will be used for the case study in this paper and will be discussed in Section 5.3.

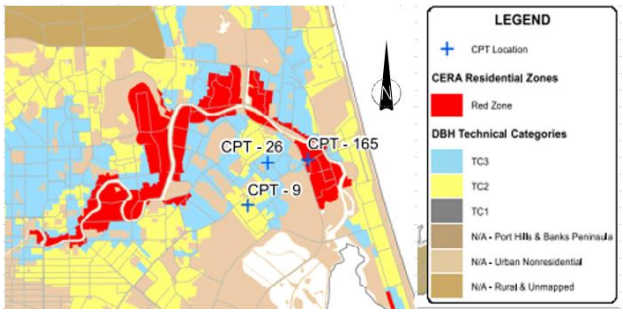

Figure 2. Land classification in Christchurch (MBIE 2012)

5.2 *Geology of Christchurch*

Prior to development of the city of Christchurch in 1850, the area was underlain by river and floodplain deposits through fluvial processes, mainly swamp land and regularly flooded by the Waimakirri River. The younger, post-glacial, deposits are about 15 to 40 m thick overlaying the Riccarton Gravel.

The alignment of the south and north branches of the Waimakirri river have changed over time, creating upper geological formations (Cubrinovski et al. 2010) that are young, loose and contain soft sediments with shallow groundwater. These young sediments contributed to widespread liquefaction, lateral spreading and settlement during major earthquakes.

5.3 *CPT data*

Figure 3 presents the CPT profiles at the residential red zone (CPT-165) and at TC3 (CPT-26). The CPT dat at TC2 (CPT-9) is shown in Figure 4.

The depths of all CPTs are 20 m and the groundwater level recorded during the tests are at 1.4 m, 2.5 m and 2 m below ground surface for CPT-165, CPT-26 and CPT 9, respectively.

5.4 *Design Earthquake*

The assessment of liquefaction triggering depends on the level of earthquake shaking. Two parameters affecting this are the peak ground acceleration (PGA) and earthquake magnitude (Mw).

Table 3 summarizes earthquake demands for liquefaction triggering analysis in the Canterbury area based on the MBIE 2015 guidelines (Tonkin & Taylor 2015).

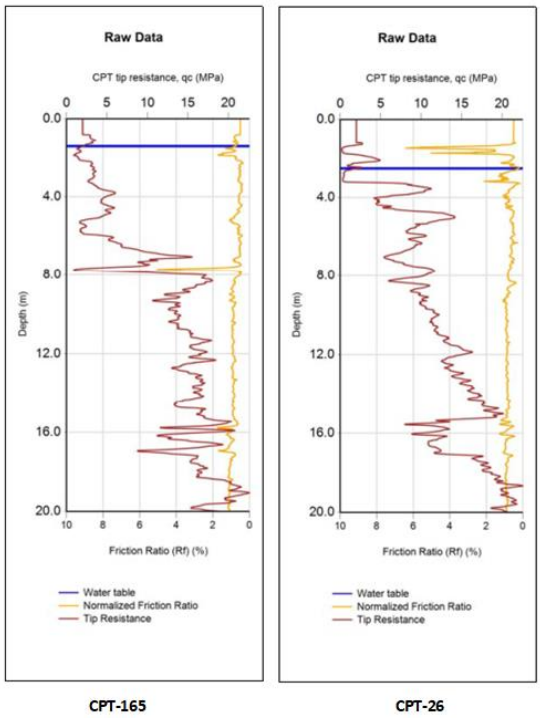

Figure 3. CPT-165 and CPT-26

Table 3. Earthquake demands for liquefaction triggering analysis

Design case	Annual probability of exceedance	PGA at Mw = 7.5	PGA at Mw = 6.0
SLS	1 in 25 years	0.13g	0.19g
ILS	1 in 100 years	0.20g	0.30g
ULS	1 in 500 years	0.35g	0.52g

SLS = Serviceability limit state
ILS = Intermediate level of shaking

ULS = Ultimate limit state

PGA and Mw values are considered as deterministic variables in this study.

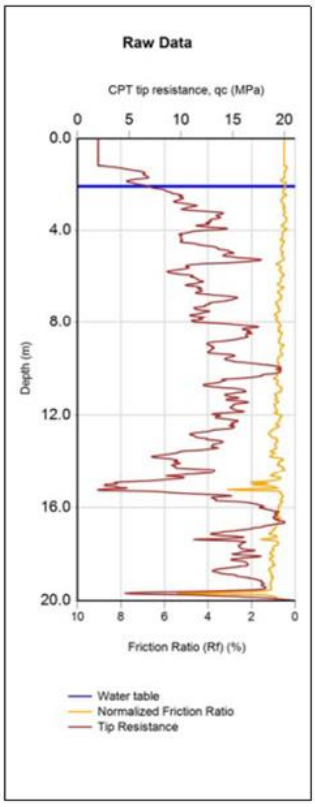

Figure 4. CPT-9

5.5 *Random variables*

As the main objective of this study is to introduce an application of the reliability-based approach for assessing liquefaction vulnerability, the field data (i.e. CPT) are assumed to be random variables and discretized into thin layers.

The following non-liquefying crust depths have been assumed in the analysis, 0.8 m, 1.2 m, and 1.2 m for CPT-165, CPT-26 and CPT 9, respectively.

The other random variables considered in this study are summarised in Table 4 below. There are twenty-three (23) random variables assumed to have normal distributions.

Table 4. Random variables

Random variables	Description	Mean values	Standard deviation
q_c *(MPa)*	Cone resistance[1]	CPT data	30%
γ *(kN/m^3)*	Soil unit weight	18	1
h_w (m)	Groundwater level[2]	1.4	1
ε	Correction for fine content[3]	0.07	0.15

1. Each CPT is subdivided into 20 sub-layers which thickness are between 0.7 m to 1.2 m based on soil classification. As cone reading can be affected by layers above or below, spatial correlation by assuming an autocorrelation distance, δ, of 0.5 m is considered in the analysis (refer Eq. 13 below).
2. Groundwater is measured from ground surface.
3. Correction for fine content (refer to Eq. 8).

The spatial correlation of cone resistance, ρ_{ij}, is based on the following established negative exponential model (Low 2003).

$$\rho_{ij} = e^{-\frac{|Depth(i)-Depth(j)|}{\delta}} \quad (13)$$

5.6 *Case 1 – Relationship between Cumulative Distribution Function (CDF) and LPI*

Case 1 is to define the relationship between the CDF and LPI for each CPT data point under an earthquake event. The ILS design earthquake of Mw = 7.5 and PGA = 0.2g was chosen for this case.

The limit state boundary is a targeted LPI value. A few LPI values are analyzed independently with the given random variables presented in Table 4. By carrying out a series of analyses with different LPI values, the CDF for each CPT can be produced based on the following:

- When the chosen LPI value is smaller than the mean LPI value, minimize reliability index, β as in Eq. 12. $P[F > F_{LimitState}] \sim \Phi(-\beta)$, where $\Phi(.)$ is the standard normal cumulative distribution function. Note that the mean value generally is close to the deterministic LPI value.
- When the chosen LPI value is larger than the mean LPI value, maximize reliability index, β. $P[F > F_{LimitState}] \sim \Phi(\beta)$, where $\Phi(.)$ is the standard normal cumulative distribution function.

Note that due to highly nonlinear expressions involved in the analysis, selection of initial values of random variables are an important stage to find an optimal result.

The CDF plots and corresponding values of β with respect to LPI for each CPT are presented in Figure 5.

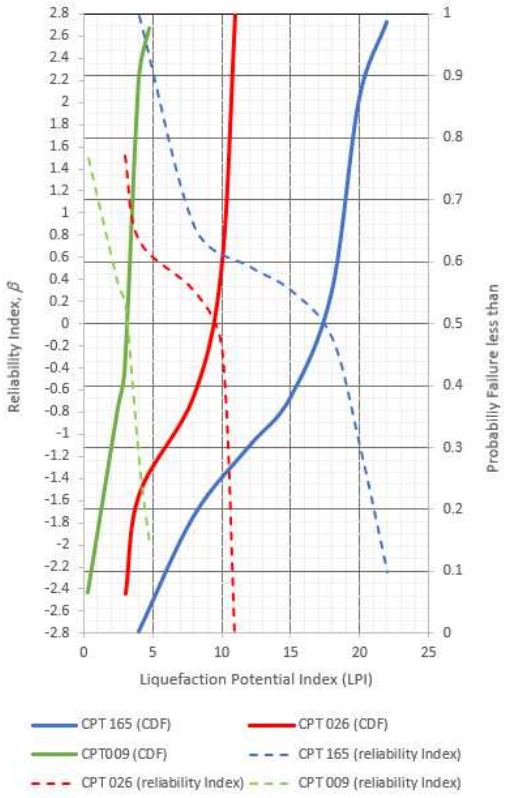

Figure 5. CDF plots obtained from reliability indices

The CDF curve for CPT-165 shows that severe liquefaction causing potential major damage to property and land is likely to occur in this area, as there is a 62% probability that the LPI will be above 15 (refer Table 1). This result confirms the classification of the area to be in the red zone (refer Figure 2).

The CDF curve for CPT-026 shows that moderate liquefaction is predicted in this area with LPI values always below 11 (refer Table 1). The median LPI value is 9 and referring to Table 2, the land is classified within technical category TC3.

The CDF curve for CPT-009 shows that probability of liquefaction is low or marginal in this area with LPI always less than 5. This confirms that the land should be classified within technical category TC2 (refer Table 2).

5.7 *Case 2 – LPI Probability of LPI under different earthquake events*

Case 2 is to compare the LPI probability of a site under different earthquake events. This study only focuses on the most critical site that is represented by CPT-165. The ILS and ULS design cases were considered.

In this section β values are specified to determine LPI values with the random variables provided in Table 4. The chosen β values are 0.3 and 0 that correspond to LPI probability of 38% or less and 50% or less, respectively. Note that $\beta = 0$ theoretically corresponds to mean value of LPI. A nonlinear programming analysis was carried out by minimizing LPI subject to a given β.

The results are summarized in Table 5. The results show that even under an intermediate level of earthquake (ILS), the area represented by CPT-165 (red zone) is likely to experience severe liquefaction that causes potential major damage to property and land. It was predicted with $\beta = 0.3$ or 38% probability, LPI values are under 15. It is also noted that the two earthquake loading scenarios (Mw 7.5 – 0.2 g and Mw 6.0 – 0.3g) give similar outcomes.

Under the ULS design cases, the calculated LPI are 30 or over. This indicates that liquefaction causing severe damage to property and land is likely to occur in this area.

Table 5. LPI values with respect to β

Design Case	Annual probability of exceedance	Earthquake demand	LPI $\beta = 0.3$	LPI $\beta = 0.0$
ILS	1 in 100 years	Mw7.5 – 0.2g	15	18.7
ILS	1 in 100 years	Mw6.0 – 0.3g	14.9	18.1
ULS	1 in 500 years	Mw7.5 – 0.35g	31.4	35.2
ULS	1 in 500 years	Mw6.0 – 0.52g	29.8	33.1

6 CONCLUSIONS

The results presented in this paper demonstrate that the proposed probabilistic approach, coupled with a liquefaction triggering procedure, is an efficient method to determine the probability of liquefaction vulnerability represented by liquefaction potential index (LPI)

The basic procedure for the proposed approach is to minimize the reliability index with respect to chosen random variables and satisfy a limit state surface represented by a targeted LPI value. By carrying out a series of analyses with different LPI values, a CDF curve with respect to LPI can be produced. Then, by comparing the CDF curve with the threshold LPI values, liquefaction vulnerability of a site can be predicted.

Since the object-oriented constrained optimization required in this approach can be solved with readily available software (e.g. Microsoft® Excel, Matlab etc.), the application of the proposed approach can be expanded further in future including incorporating other methods of liquefaction vulnerability (e.g. LSN), spatial variability and other random variables (e.g. SPT).

7 REFERENCES

Boulanger R.W. and Idriss I.M. 2014. *CPT and SPT based liquefaction triggering procedures*. Report No. UCD/CGM-14/01, Center for geotechnical modeling, Dept. Civil and Env. Eng. University of California at Davis, California.

Canterbury Earthquake Recovery Authority (CERA). 2012. *Canterbury land information map Kaiapoi Lakes to Governors Bay.* 23rd March 2012.

Cetin K.O., Der Kiureghian A., and Seed R.B. 2002. Probabilistic models for the initiation of seismic soil liquefaction. *Structural Safety* 24, 67-82.

Cubrinovski M., Green R., Allen J., Ashford S., Bowman E., Bradley B.A., Cox B., Hutchinson T., Kavazanjian E., Orense R., Pender M., Quigley M., and Wotherspoon L. 2010. *Geotechnical reconnaissance of the 2010 Darfield (New Zealand) earthquake*. University of Canterbury, Christchurch, 173.

Ditlevsen O. 1981. *Uncertainty modeling: with applications to multidimensional civil engineering systems*. McGraw-Hill, New York.

Idriss I.M. and Boulanger R.W. 2006. Semi-empirical procedures for evaluating liquefaction potential during earthquakes. *Soil dynamics and earthquake engineering* 26, 115-130.

Idriss I.M. and Boulanger R.W. 2008. *Soil liquefaction during earthquakes*. Monograph MNO-12, Earthquake Engineering Research Institute, Oakland, CA, 261.

Ishihara K. 1985. Stability of natural deposits during earthquakes. Proc. 11th *Int. Conf. Soil Mechanics and Foundation Eng*. San Francisco, CA, USA, 1, 321-376.

Iwasaki T., Tatsuoka F., Tokida K., and Yasuda S. 1978. A practical method for assessing soil liquefaction potential based on case studies at various sites in Japan. Proc. 2nd *Int. Conf. on Microzonation*. San Francisco, CA, USA, 885-896.

Low B.K. 2003. Practical Probabilistic Slope Stability Analysis. *Proc. 12th Panamerican Conf. on Soil Mechanics and Geotechnical Engineering*, Cambridge, Massachusetts, USA, Vol. 2, 2777-2784.

Low B.K. and Tang W.H. 1997. Automated reliability based design of footing foundations. *Proc. 7th Int. Conf. on Structural Safety and Reliability*, ICOSSAR '97, Kyoto, Japan, Vol. 3, 1837-1840.

Low B.K., Teh C.I., and Tang W.H. 2001. Efficient reliability-based design using spreadsheet optimization. *Proc of the 8th Int. Conf. on Structural Safety and Reliability*, ICOSSAR '01, Newport Beach, California.

Maurer B.W., Green R.A., and Taylor O.S. 2015. Moving towards an improved index for assessing liquefaction hazard: Lessons from historical data. *Soils and Foundations* 55(4), 778-787,

Ministry of Business, Innovation and Employment (MBIE). 2012. *Repairing and rebuilding houses affected by the Canterbury earthquakes*. http://www.building.govt.nz/guidance-on-repairs-after-earthquake.

Ministry of Business, Innovation and Employment (MBIE). 2015. *Repairing and rebuilding houses affected by the Canterbury earthquakes – Section 15.3 updated guidance on site ground improvement, Christchurch*.

Moss R.E.S., Seed R.B., Kayen R.E., Stewart J.P., Der Kiureghian A. and Cetin K.O. 2006. *J. Geotechnical and Geoenvironmental Engineering ASCE*, 132(8), 1032-1051.

Robertson P.K. and Wride C.E. 1998. Evaluating cyclic liquefaction potential using the cone penetration test. *Canadian Geotech. Journal*, 35(3), 442-459.

Seed H.B. and Idriss I.M. 1971. Simplified procedure for evaluating soil liquefaction potential. *J. Soil Mechanics and Foundations Div. ASCE,* 97(SM9), 1249-1273.

Tandjiria V., Teh C.I., and Low B.K. 2000. Reliability analysis of laterally loaded piles using response surface methods. *Structural Safety* 22, 335-355.

Tonkin & Taylor Ltd. 2013. *Liquefaction vulnerability study*. T&T Ref: 52020.0200/v1.0.

Tonkin & Taylor Ltd. 2015. *Canterbury earthquake sequence: increased liquefaction vulnerability assessment methodology*. T&T Ref: 52010.140/v1.0.

Zhang G., Robertson P.K. and Brachman R.W.I. 2002. Estimating liquefaction-induced ground settlements from CPT for level ground. *Canadian Geotechnical Journal* 39, 1168-1180.